Unambiguous quantum measurement of nonorthogonal states

B. Huttner, A. Muller, J. D. Gautier, H. Zbinden, and N. Gisin
Group of Applied Physics, University of Geneva, CH-1211, Geneva 4, Switzerland
(Received 17 April 1996)

Generalized quantum measurements can be used to separate deterministically two nonorthogonal quantum states. However, such measurements also lead to inconclusive results, where the initial state remains unknown. We introduce a particular type of generalized quantum measurement, which we term loss induced generalized (LIGe) quantum measurement, and present an experimental realization. This LIGe measurement achieves optimal deterministic separation of two nonorthogonally polarized single photons. [S1050-2947(96)01311-X]

PACS number(s): 03.65.Bz, 42.81.Gs

I. INTRODUCTION

Let us assume that you are given spin-$\frac{1}{2}$ particles in one of two nonorthogonal states, say, $|\psi_1\rangle$ or $|\psi_2\rangle$, satisfying

$$|\langle\psi_1|\psi_2\rangle| \equiv \cos\alpha \neq 0 \tag{1}$$

and with the same *a priori* probability.[1] For each particle, your task is to try to identify the preparation. Rushing through your lecture notes from your quantum mechanics course [1], you quickly realize that it is impossible to achieve your goal: two nonorthogonal states cannot be distinguished with certainty. In fact, if you restrict yourself to standard quantum measurements (also known as Von Neuman measurements [2]), the best you can do is to project your states onto two orthogonal states $|\phi_1\rangle$ and $|\phi_2\rangle$, chosen to be ''as close as possible'' to the original states, while keeping the orthogonality condition (see Fig. 1). The result of your measurement will be either $|\phi_1\rangle$ or $|\phi_2\rangle$, which you will identify with $|\psi_1\rangle$ and $|\psi_2\rangle$, respectively [3]. This setup gives you a probability of error

$$q \equiv \mathrm{Prob(error)} = |\langle\psi_1|\phi_2\rangle|^2 = |\langle\psi_2|\phi_1\rangle|^2 = \frac{1}{2}(1-\sin\alpha)\ . \tag{2}$$

If you had no *a priori* information on the initial state, the initial entropy of your system was $H_{\mathrm{ini}}=1$ (in bits). After your measurement, with a probability of error q, the entropy becomes $H_{\mathrm{fin}}=-q\log_2 q-(1-q)\log_2(1-q)$, where we use the base 2 logarithm ($\log_2$) to obtain the entropy in bits. The average information gain (in bits) given by this measurement strategy is

$$I_{\mathrm{vN}} \equiv H_{\mathrm{ini}} - H_{\mathrm{fin}} = 1 + q\log_2 q + (1-q)\log_2(1-q). \tag{3}$$

It is well known that this is the best you can do in terms of information gain [4,5].[2]

However, in some cases, this may not be the optimal measurement for your particular purposes. For example, your loss may be so high if you make the wrong decision that what you require is not to gain the maximum information, but rather to avoid making any mistake. It is slightly less well known that quantum mechanics still allows you to do so [7,8]. Instead of having a binary answer, either $|\psi_1\rangle$ or $|\psi_2\rangle$, with a given probability of error, you add a third possibility, known as an inconclusive result. At the end of your test, you therefore know with certainty that the particle was either in state $|\psi_1\rangle$ or in state $|\psi_2\rangle$, or that you do not know the initial state. A simple way to implement this test is to choose at random whether to project your particle onto $|\psi_1^{\perp}\rangle$, orthogonal to $|\psi_1\rangle$, or onto $|\psi_2^{\perp}\rangle$. If you choose to project onto $|\psi_1^{\perp}\rangle$ and get a positive result, you know that the initial state could not have been $|\psi_1\rangle$ and was therefore $|\psi_2\rangle$. If you get a negative result, you cannot make a deterministic conclusion: the state may have been either. In order to avoid making a wrong decision, you simply discard the measurement and call the result inconclusive (it is obvious that there is still information left in the inconclusive results, which means that this simple procedure is not optimal; we will present an optimal setup in the following). This particular scheme is a somewhat trivial example of a generalized quantum measurement. This type of measurement, also known as positive operator-valued measure (POVM) [3,7,9], cannot be reduced to standard projections of the initial state onto orthogonal states spanning the initial Hilbert space alone. Our example already shows that, in some cases, they may be preferable to a standard quantum measurement.

In Sec. II we shall first give a brief theoretical overview on generalized measurements, followed by the introduction of a particular type of measurement, which we term the loss induced generalized (LIGe) measurement. In Sec. III we

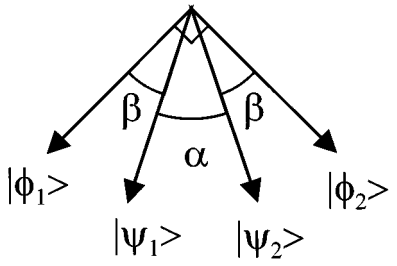

FIG. 1. Standard projection measurement of two nonorthogonal states $|\psi_1\rangle$ and $|\psi_2\rangle$, verifying $\langle\psi_1|\psi_2\rangle=\cos\alpha$. These states are projected onto the two orthogonal states $|\phi_1\rangle$ and $|\phi_2\rangle$ ($\beta=\pi/4-\alpha/2$).

[1]This restriction is not necessary, but will be adopted in this work to simplify the algebra.

[2]Note that this is not true in higher dimensions: a standard measurement need not give the highest information gain [4,6].

present our system for implementing such a measurement using polarized single photons. Our measurement strategy achieves the theoretical optimum for separating nonorthogonally polarized single photons. In Sec. IV we show the experimental realization and present our results. We finally conclude in Sec. V.

II. QUANTUM MEASUREMENTS

A. Standard measurements

Returning to our lecture notes on quantum mechanics, or to any good textbook [1], we discover that any measurable physical quantity, say $\mathcal{A}$, is represented by a Hermitian operator A in our Hilbert space H, known as an observable. The main property of an observable is that it has a complete set of eigenvectors. Moreover, two eigenvectors corresponding to different eigenvalues are orthogonal. In an n-dimensional Hilbert space, we can write the completeness condition as

$$\sum_{i=1,\ldots,n} P_i = \mathbb{1}, \tag{4}$$

where P_i is the projection operator on eigenvector $|\phi_i\rangle$ and $\mathbb{1}$ is the identity operator. A measurement of the physical quantity $\mathcal{A}$ can only give one of the eigenvalues of A and the initial state $|\psi\rangle$ is projected onto the corresponding eigenvector. Such a measurement is also known as an orthogonal measurement [10]. The probability of obtaining the result i is given by the overlap with the corresponding eigenstate

$$p(i) = |\langle \phi_i | \psi \rangle|^2. \tag{5}$$

More generally, if the initial state is described by a density matrix ρ, the probability becomes

$$p(i) = \mathrm{Tr}(\rho P_i), \tag{6}$$

which reduces to Eq. (5) for a pure state.

B. Generalized measurements

The above notion of quantum measurements is, however, too restrictive. For example, it was shown by Benioff [11] that, in general, a succession of two such measurements cannot be represented by a single standard measurement. A more general measurement is not a direct projection onto a set of orthogonal states, but involves coupling the system under consideration to an auxiliary one, known as an ancilla. This is followed by a standard measurement of either the ancilla alone or the global system [3,10,12]. Mathematically, this type of measurement can also be defined in terms of the original Hilbert space alone, by a generalization of Eq. (4). Instead of describing it in terms of a set of orthogonal projection operators P_i, the generalized measurement can be described by a number of, possibly noncommuting, positive operators Q_i, which satisfy

$$\sum_{i=1,\ldots,m} Q_i = \mathbb{1}, \tag{7}$$

where m can now be larger than the dimension of the Hilbert space. As the Q_i are not orthogonal projection operators, such a measurement is sometimes known as a nonorthogonal measurement [10]. This is the type of measurement that we need for the problem discussed in the Introduction: even though we are in a two-dimensional Hilbert space, we need a measurement with three possible answers: the state was $|\psi_1\rangle$; the state was $|\psi_2\rangle$; or the state is unknown. The probability of obtaining the result i is given by

$$p(i) = \mathrm{Tr}(\rho Q_i), \tag{8}$$

where ρ is the density matrix of the initial state.

The link between the formal description of Eq. (7) and the more physical introduction of an ancilla followed by a standard orthogonal measurement is given by the Neumark theorem [3,12,13]. This theorem states that any generalized measurement described by Eq. (7) can be obtained from an orthogonal measurement in a higher-dimensional space. The choice of either description is therefore more or less a matter of convenience. However, two points are worth emphasizing.

(i) In the laboratory, the result given by a measuring device is always one in a set of macroscopically distinguishable states (e.g., the position of a meter or a number of counts in a counter). Therefore, the final states of at least the apparatus are necessarily orthogonal. So the physical description of the measurement needs to include an orthogonal projection.

(ii) The description in terms of noncommuting operators Q_i is incomplete in the sense that it does not specify uniquely the state of the system after the measurement. In fact, this state depends on the exact implementation in terms of an ancilla [14].

Therefore, in the following, we shall mainly use the more physical picture and describe our generalized measurement in terms of orthogonal projections in a higher-dimensional Hilbert space.

C. Geometrical representation

Let us return to the example given in the Introduction of two nonorthogonal states $|\psi_1\rangle$ and $|\psi_2\rangle$, as shown in Fig. 1. The two-dimensional Hilbert space spanned by the system can be embedded in a three-dimensional (3D) space. The third dimension is given by the state $|\phi_0\rangle$, orthogonal to the two initial states. This is described in Fig. 2. We first perform a unitary evolution of the system in the 3D space. Geometrically, this evolution, denoted by U, is a rotation in 3D around vector $|u_1\rangle \equiv (1/\sqrt{2})(|\phi_1\rangle - |\phi_2\rangle)$, with angle θ. It is easy to see that the initial state $|\psi_1\rangle$ is transformed into

$$\begin{aligned} U|\psi_1\rangle = {} & \frac{1}{\sqrt{2}}\left(\sin\frac{\alpha}{2} + \cos\frac{\alpha}{2}\cos\theta\right)|\phi_1\rangle \\ & + \frac{1}{\sqrt{2}}\left(-\sin\frac{\alpha}{2} + \cos\frac{\alpha}{2}\cos\theta\right)|\phi_2\rangle \\ & + \cos\frac{\alpha}{2}\sin\theta|\phi_0\rangle, \end{aligned} \tag{9}$$

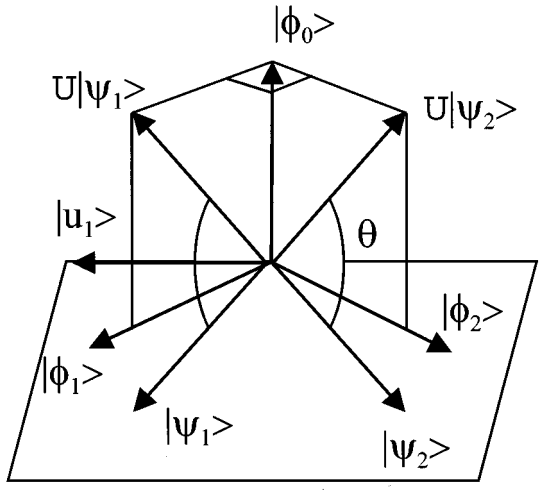

FIG. 2. Geometrical representation of a generalized measurement. The initial 2D Hilbert space is embedded into a 3D space by adding an extra state $|\phi_0\rangle$, which is orthogonal to the two initial states. The measurement consists of one rotation U around vector $|u_1\rangle$ with angle θ, followed by a standard projection measurement in the 3D space onto the three orthogonal vectors $|\phi_0\rangle$, $|\phi_1\rangle$, and $|\phi_2\rangle$. Vector $|\psi_1\rangle$ is transformed into $U|\psi_1\rangle$, which is orthogonal to $|\phi_2\rangle$, and reciprocally for $|\psi_2\rangle$.

while the initial state $|\psi_2\rangle$ is transformed into

$$U|\psi_2\rangle=\frac{1}{\sqrt{2}}\left(-\sin\frac{\alpha}{2}+\cos\frac{\alpha}{2}\cos\theta\right)|\phi_1\rangle+\frac{1}{\sqrt{2}}\times\left(\sin\frac{\alpha}{2}+\cos\frac{\alpha}{2}\cos\theta\right)|\phi_2\rangle+\cos\frac{\alpha}{2}\sin\theta|\phi_0\rangle. \tag{10}$$

The angle of rotation θ is chosen to be

$$\cos\theta=\tan\frac{\alpha}{2}, \tag{11}$$

which gives

$$U|\psi_1\rangle=\sqrt{2}\sin\frac{\alpha}{2}|\phi_1\rangle+\sqrt{\cos\alpha}|\phi_0\rangle, \tag{12}$$

$$U|\psi_2\rangle=\sqrt{2}\sin\frac{\alpha}{2}|\phi_2\rangle+\sqrt{\cos\alpha}|\phi_0\rangle. \tag{13}$$

Since the three states $|\phi_0\rangle$, $|\phi_1\rangle$, and $|\phi_2\rangle$ are orthogonal, it is possible to separate them deterministically with a standard measurement. For initial state $|\psi_1\rangle$, the result of the measurement can be either $|\phi_1\rangle$, with probability $2\sin^2\alpha/2$, or $|\phi_0\rangle$, with probability $\cos\alpha$, but it cannot be $|\phi_2\rangle$, and conversely for initial state $|\psi_2\rangle$. Therefore, this system implements the unambiguous identification of the two initial states. The probability of obtaining an inconclusive result is

$$p(?)=\cos\alpha. \tag{14}$$

This is indeed the optimal that can be achieved for two states with overlap $|\langle\psi_1|\psi_2\rangle|=\cos\alpha$ [12,15].

D. Formal definition of a LIGe measurement

We now expand the previous discussion to higher-dimensional space and formally define a LIGe measurement. We start with a system in a p-dimensional space $\mathcal{H}_S$, which we embed in a larger N-dimensional space $\mathcal{H}_T$. This can be done, for example, by explicitly introducing an ancilla and performing the tensor product with $\mathcal{H}_S$. The space $\mathcal{H}_S\otimes|a_0\rangle$, where $|a_0\rangle$ is the initial state of the ancilla, is then a subspace of the total space $\mathcal{H}_T$. A generalized measurement on the system consists first of a unitary transformation U in $\mathcal{H}_T$, followed by a standard measurement.[3] An initial state, which may be characterized by its density matrix $\rho_{\rm in}$, is first transformed into $U\rho_{\rm in}U^\dagger$. The measurement then corresponds to projections onto one of the N orthogonal states: $|\phi_1\rangle,\ldots,|\phi_N\rangle$. The probability to get the result i is

$$p(i)=\mathrm{Tr}(U\rho_{\rm in}U^\dagger|\phi_i\rangle\langle\phi_i|)=\mathrm{Tr}(\rho_{\rm in}U^\dagger|\phi_i\rangle\langle\phi_i|U). \tag{15}$$

Therefore, the set of operators P_i corresponding to this measurement (see Sec. II A) is given by

$$P_i=U^\dagger|\phi_i\rangle\langle\phi_i|U. \tag{16}$$

For reasons that shall become clear in the following, we define a LIGe measurement as a measurement for which the first p vectors $|\phi_1\rangle,\ldots,|\phi_p\rangle$ are inside $\mathcal{H}_S$ (this implies that the other vectors are in $\mathcal{H}_S^\perp$). We group all the other vectors together and consider this result as inconclusive. In this case, it is possible to express the measurement in $\mathcal{H}_S$ alone as a nonunitary transformation, followed by a standard measurement projecting on the vectors $|\phi_1\rangle,\ldots,|\phi_p\rangle$. For initial state $|\psi\rangle$, the transformation gives

$$|\psi\rangle\rightarrow PU|\psi\rangle, \tag{17}$$

where P is the orthogonal projection on $\mathcal{H}_S$. The transformation PU is known as a contraction [16] from $\mathcal{H}_T$ to $\mathcal{H}_S$. It is also possible to define a nonunitary transformation T *within* $\mathcal{H}_S$[4] by

$$T=PUP. \tag{18}$$

It is easily seen that this transformation is diagonalizable and has eigenvalues with a modulus bounded by one. Therefore, it can be written as

$$T=e^{-iH-A}=e^{-iH}e^{-A}, \tag{19}$$

where H and A are two commuting Hermitian operators and A is positive. The operator e^{-A} represents the losses in the system. Indeed, the transformation T does not conserve the norm, but introduces state-dependent losses. Following the

[3]It is also possible to perform the standard measurement directly in $\mathcal{H}_T$ without any unitary transformation first. We prefer to keep these two stages as this corresponds more closely to the experimental situation where the system is first coupled to a measuring apparatus and then measured.

[4]Formally, T is a $N\times N$ matrix, but it has zeros everywhere, except in the leading $p\times p$ block, and so can be considered as a transformation within $\mathcal{H}_S$.

demonstration leading to Eqs. (15) and (16) and replacing U by T, we can write the family of operators corresponding to the LIG measurement as Q_i, $i=1,\ldots,p$, with

$$Q_i = T^\dagger |\phi_i\rangle\langle\phi_i| T, \tag{20}$$

which give the conclusive results, and

$$Q_{p+1} = 1 - \sum_{i=1}^{p} Q_i = 1 - e^{-2A}, \tag{21}$$

which gives the inconclusive result. Since A is positive, all these operators are positive. Following the results of Sec. II B, Eqs. (20) and (21) therefore define a POVM.

This rather abstract formalism can be made clearer by using the previous example of Sec. II C. Here U is a 3D rotation, which is followed by an orthogonal measurement along the three vectors $|\phi_0\rangle$, $|\phi_1\rangle$, and $|\phi_2\rangle$. As both $|\phi_1\rangle$ and $|\phi_2\rangle$ are in the initial two-dimensional Hilbert space $\mathcal{H}_S$, this is a LIG measurement. It is easy to obtain the explicit expression for T acting on $|\phi_1\rangle$ and $|\phi_2\rangle$:

$$T|\phi_{1,2}\rangle = \frac{1}{\sqrt{2}\cos\left(\frac{\alpha}{2}\right)} |\psi_{2,1}^{\perp}\rangle, \tag{22}$$

where $|\psi_1^{\perp}\rangle$ and $|\psi_2^{\perp}\rangle$ are the normalized vectors orthogonal to $|\psi_1\rangle$ and $|\psi_2\rangle$, as defined in Sec. I. The norm of $T|\phi_{1,2}\rangle$ is less than one, which means that T introduces loss in the system. We can also write the projection operators Q_i,

$$Q_{1,2} = \frac{1}{2\cos^2\left(\frac{\alpha}{2}\right)} |\psi_{2,1}^{\perp}\rangle\langle\psi_{2,1}^{\perp}| \tag{23}$$

and

$$Q_3 = 1 - Q_1 - Q_2. \tag{24}$$

This shows how the more physical picture of a POVM as a coupling between the system and an auxiliary one is related to the mathematical definition of a POVM in terms of noncommuting operators in the initial space. We now turn to a practical implementation of this type of measurement.

III. THEORETICAL MODEL FOR LIGe MEASUREMENT

A. Macroscopic regime

The setup for a practical LIGe measurement is shown in Fig. 3. Let us first examine it in the macroscopic regime, with classical electromagnetic fields. We shall consider two incoming states, linearly polarized with angles $\pm\eta$ with respect to the vertical axis. An incoming field is split by a polarization beam splitter (PBS1) into horizontal and vertical components. The horizontal polarization continues on a straight line, while the vertical one is deviated at 90°. The vertical branch is attenuated by a beam splitter (BS1), with a transmission coefficient t. The two branches are then recombined at a second PBS (PBS2). The optical paths of the two branches are adjusted to be equal. When the transmission coefficient t is chosen to be

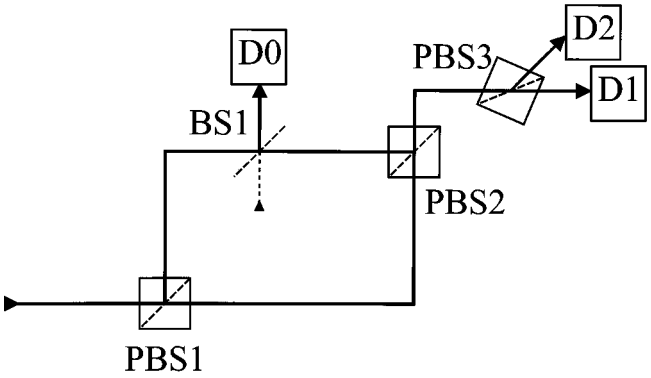

FIG. 3. Setup of an optimal LIGe measurement of the polarization of single photons. The incoming beam is split by a polarization beam splitter (PBS1) into horizontal and vertical components. Part of the vertical component is attenuated at a beam splitter (BS1) and the two are then recombined at PBS2. Two states with polarization $\pm\eta$ with respect to the vertical axis are transformed into orthogonal states, with polarization at $\pm 45°$, and can be deterministically separated at PBS3.

$$t = \tan\eta, \tag{25}$$

the two fields at $\pm\eta$ are transformed into two orthogonally polarized fields oriented at $\pm 45°$, and can be easily separated by PBS3 (as shown in Fig. 3).

The above setup enables us to take two nonorthogonally polarized fields and transform them into two orthogonally polarized ones, at the expense of introducing some attenuation. We shall now turn to the quantum regime and analyze the same setup with single photons.

B. Quantum regime

The two states we shall consider are nonorthogonally polarized single-photon states. We choose our basis for the polarization as the vertical and the horizontal axis and use the usual Fock space representation [17] to denote the corresponding states by $|1,0\rangle$ for the horizontal polarization (there is one photon in the horizontal mode and zero in the vertical one) and by $|0,1\rangle$ for the vertical polarization. The two single-photon states polarized at $\pm\eta$ with respect to the vertical axis are then given by

$$|\psi_1\rangle = \cos\eta|0,1\rangle + \sin\eta|1,0\rangle, \tag{26}$$

$$|\psi_2\rangle = \cos\eta|0,1\rangle - \sin\eta|1,0\rangle, \tag{27}$$

which gives an overlap $\langle\psi_1|\psi_2\rangle = \cos 2\eta$. In order to introduce BS1 in the vertical branch, we need to add the vacuum state entering at the second port of BS1, which will get coupled to the input state. The splitting is then represented by a unitary operator U, whose action on state $|0,1\rangle$ is

$$U|0,1\rangle\otimes|0\rangle = t|0,1\rangle\otimes|0\rangle + r|0,0\rangle\otimes|1\rangle, \tag{28}$$

where $\otimes$ represent the direct product of the initial space with the new mode. A photon originally in the vertical polarization mode will either remain in the same state, with amplitude t, or be transferred to the new mode, with amplitude r. If the transmission amplitude t is again chosen to be $t=\tan\eta$, we easily obtain the states after splitting:

$$U|\psi_1\rangle\otimes|0\rangle=\sqrt{2}\sin\eta|\phi_1\rangle\otimes|0\rangle+\sqrt{\cos 2\eta}|0,0\rangle\otimes|1\rangle, \tag{29}$$

$$U|\psi_2\rangle\otimes|0\rangle=\sqrt{2}\sin\eta|\phi_2\rangle\otimes|0\rangle+\sqrt{\cos 2\eta}|0,0\rangle\otimes|1\rangle, \tag{30}$$

where $|\phi_1\rangle$ and $|\phi_2\rangle$ are the two orthogonal single-photon states polarized at $\pm 45°$:

$$|\phi_1\rangle=\frac{1}{\sqrt{2}}(|0,1\rangle+|1,0\rangle), \tag{31}$$

$$|\phi_2\rangle=\frac{1}{\sqrt{2}}(|0,1\rangle-|1,0\rangle). \tag{32}$$

If we put single-photon detectors in the three output branches, we can now get the full statistics for this measurement system: a count in D1 corresponds to initial state $|\psi_1\rangle$, a count in D2 corresponds to initial state $|\psi_2\rangle$, and a count in D0 corresponds to an inconclusive result. The probability for this is $p(?)=\cos 2\eta$. This system is therefore equivalent to the one presented in Sec. II C and realizes the optimal separation of the two nonorthogonal states.

IV. EXPERIMENTAL REALIZATION

A. Setup

The appealing property of the setup suggested in the preceding section is that it enables us to obtain directly the statistics for the three possible answers: $p(\phi_1)$, $p(\phi_2)$, and $p(?)$. However, it requires an interferometer that needs to be kept stable. A much simpler setup was therefore chosen for our experiment and is presented in Fig. 4. The main element is a polarization maintaining fiber that possesses polarization-dependent losses [18]. We will refer to it as a PDL fiber. In this type of fiber, one linear polarization mode propagates without attenuation, while the orthogonal mode is attenuated (PDL fibers are usually used as polarizers: a long enough fiber completely absorbs one mode, leaving only one linear polarization at the output). This fiber replaces the interferometer of Fig. 3 [19]. The advantage is that as the two polarized states propagate in the same fiber, the stability of the experiment is much better than with two spatially separated beams. Also, since the PDL fiber enables us to modify the polarization continuously during the propagation, it is possible to change the attenuation by using different lengths of fibers. Instead of having one discrete jump, like in ordinary polarizers, we can in principle monitor the evolution of the state of the polarization [20]. The disadvantage is that we do not have access to the lossy mode anymore and so cannot get directly the probability for inconclusive results.

In this setup, the laser beam, at a wavelength of 1300 nm, is first sent through a $\lambda/4$ wave plate, followed by a rotating polarizer, which enables us to send any chosen linear polarization towards the PDL fiber, with a fixed intensity. We vary the polarization angle η, while monitoring the output intensity (after the PDL fiber), to obtain the two principal axes of the fiber. To keep the same notation as in Sec. III, we shall call the nonlossy axis horizontal and the lossy one vertical. We also choose the latter as the angular origin. If the overall attenuation coefficient in the vertical axis is t, then the two states polarized at $\pm\eta$, with $t=\tan\eta$, will become orthogonal. However, in a polarization maintaining fiber, because of the birefringence, the two modes do not propagate at the same velocity.[5] Therefore, the two output states need not be linearly polarized, but can have any elliptical polarization. In order to enable separation at a PBS, we need to add another polarization controller, which transforms the two elliptical polarizations into two linear ones. We set the controller to send the state $+\eta$, say, in detector D1 and shall get the state $-\eta$ in detector D2. The setup is first aligned and calibrated with strong pulses. Then the intensity is greatly reduced to obtain very weak pulses, with, on average, 0.1 photon per pulse. This ensures that the probability to get more than one photon in one pulse is negligible. Most pulses have no photon at all and will simply not be counted. This means that even though we do not create pure single photon states, but rather weak coherent states, we select only the cases where the initial pulse contains one photon. This justifies our theoretical approach of Sec. III B. Therefore, during the experiment, we send and detect the photons one by one.

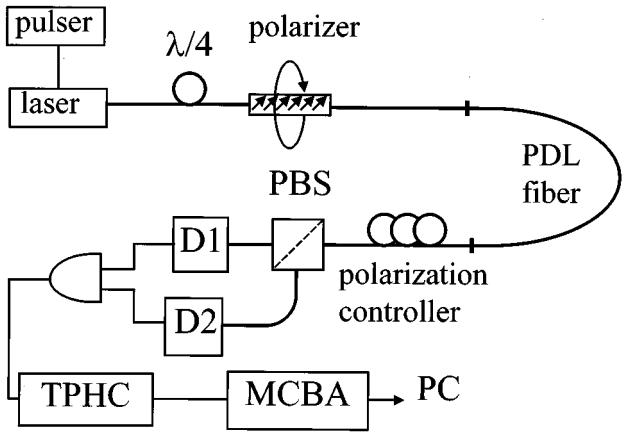

FIG. 4. Implementation of a simple LIG measurement. A pulsed laser (wavelength 1300 nm, length of the pulses about 1 ns) is strongly attenuated to obtain pulses with 0.1 photon on average. It is first transformed into a circularly polarized beam by a $\lambda/4$ plate. The following linear polarizer enables one to choose any linear polarization, with a fixed intensity. The PDL fiber plays the role of the interferometer in Fig. 3: the input state is split into the two polarization components, one of which is attenuated during the transmission. The polarization controller creates linearly polarized output states that can be separated at the PBS. The light on each side of the PBS is sent to Ge avalanche detectors D1 and D2 operating in the Geiger mode, to detect single photons. The signal is amplified, discriminated, and combined at an ''or'' gate. The time to pulse height converter (TPHC) (EGG-Ortec) records the time of arrival of each photons. The slightly different lengths in the two output ports ensure that the photons coming from the two ports arrive at different times. The multichannel buffer analyzer (MCBA) (EGG-Ortec) analyzes the amplitudes produced by the TPHC, which are then recorded in the PC.

[5]This is known as polarization mode dispersion (PMD) and exists in all optical fibers. However, PMD is much larger in polarization maintaining fibers.

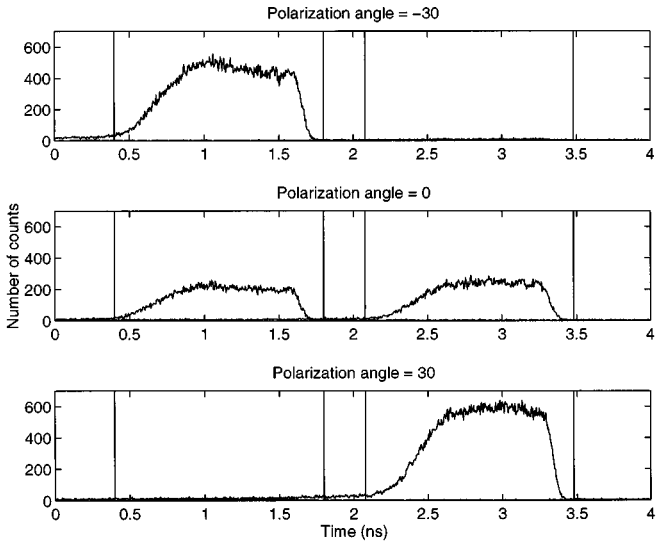

FIG. 5. Time histogram of the detected photons. The horizontal scale represents the channels in the MCBA converted in nanoseconds (one channel represents 3 ps). The vertical scale is the corresponding number of detected photons. The differential attenuation in the PDL fiber is 4.54 dB, corresponding to $\eta = 30°$. The first window corresponds to photons arriving in D1 (shorter path) and the second window to the photons arriving in D2 (longer path). (a) The input angle is $-30°$ and most photons arrive in D1, with an error rate of about 2.0% (ratio of the number of counts in D2 with respect to D1). (b) The input angle is 0° and the photons are equally split in the two ports. (c) The input angle is 30° and most photons arrive in D2, with an error rate of about 1.7%.

B. Results

The results are presented in Fig. 5. We choose a PDL fiber [18] of 25 cm, which gave a differential attenuation of 4.54 dB. Using Eq. (25), this corresponds to an angle $\eta = 30°$. The two states $|\psi_1\rangle$ and $|\psi_2\rangle$ are therefore polarized at angle $\pm 30°$ with respect to the lossy axis, which is chosen as the origin. With strong pulses, we choose light polarized at $-30°$ and adjust the polarization controller to get the maximum intensity in detector D1 and the minimum in D2. We rotate the polarization to $+30°$ and check that the intensity is now maximum in D2 and minimum in D1. We then attenuate the pulses very strongly to get about 0.1 photon per pulse on average and go to photon counting. The detectors were Ge avalanche photodiodes, operating in the Geiger mode [21]. When the initial state is $|\psi_1\rangle$, the number of counts is maximum in D1 and minimum in D2 [Fig. 5(a)]. The error rate (ratio of counts in D2 over D1) is 2%. When the initial state is along the lossy axis [Fig 5(b)], there is roughly the same number of counts in both detectors (the difference is due to an unbalance between the two ports, together with a slightly different efficiency of the detectors). With initial state $|\psi_2\rangle$, the number of counts in D2 is now maximum and in D1 minimum. The error rate here is 1.7%. In contrast, the *theoretical* error rate given by a standard projection measurement, corresponding to an overlap $\langle\psi_1|\psi_2\rangle = \cos 2\eta$, is about 6.7% [from Eq. (2)]. This shows that our LIGe measurement can indeed separate the two nonorthogonal states in a better fashion than even the optimal projection measurement with no experimental noise at all.

V. CONCLUSION

In this paper we have shown that generalized quantum measurements, where the system under consideration is coupled to an auxiliary quantum system (the ancilla) before performing a standard projection measurement on the full system, are not a mathematical curiosity, but can indeed be implemented in the laboratory. We specifically introduced and performed a LIGe quantum measurement to demonstrate this point. This type of generalized measurement is interesting because, on the one hand, it is easily performed in the laboratory (the auxiliary system being simply an extra degree of freedom in the vacuum state, which is coupled to the original system), while, on the other hand, its results are not obtainable with a standard measurement. Our measurement, for example, enabled us to separate two quantum states with overlap 1/2 with only about 2% error rate. The price to pay was of course that many measurement results were inconclusive, corresponding to the absorption of the photon.

One could argue that our measurement is not a purely quantum effect, in the sense that it can be understood in terms of macroscopic fields as well: two nonorthogonally polarized fields are transformed into orthogonally polarized ones, at the expense of losing part of the fields. However, an implementation with single photons is somewhat similar to well-known interferometric experiments with single photons, where the interference pattern is built from one detection at a time. Here the counterintuitive feature is that a single photon is not only split coherently into the two polarization components, but also ''knows'' that it went through an absorbing medium even though it was not absorbed. The use of a PDL fiber is also interesting because the evolution of the polarization in the fiber is continuous. On the one hand, for all the photons that were eventually detected, there was no real absorption in the fiber. On the other hand, the polarization component along the lossy axis was, nevertheless, slowly reduced, thus rotating the initial states $|\psi_1\rangle$ and $|\psi_2\rangle$ towards the orthogonal states $|\phi_1\rangle$ and $|\phi_2\rangle$.

Another somewhat counterintuitive feature is that LIGe measurements show that a well-chosen dissipative environment need not be damaging. Indeed, at least in this particular case, losses in the measurement were utilized to obtain a better separation of the two initial states. This may be put in parallel with a recent theoretical work [22], where polarization dependent losses were shown to increase quantum correlations, thus revealing hidden quantum nonlocality in pairs of spin-$\frac{1}{2}$ particles. These observations may have bearings upon the burgeoning field of quantum computation, where the interaction with a dissipative environment is generally considered as the main difficulty for realizing a quantum computer. Finally, this type of measurement may have practical applications in quantum cryptography (for an introduction see, e.g., [23]), which specifically makes use of nonorthogonal states to establish a secret cryptographic key between two users.

ACKNOWLEDGMENTS

We would like to thank G. Brassard, I. Percival, and J. Rarity for useful discussions and the Swiss Fonds National de Recherche Scientifique for financial support.

[1] C. Cohen-Tannoudji, B. Diu, and F. Laloë, *Quantum Mechanics* (Wiley, Paris, 1977).
[2] J. von Neumann, *Mathematische Grundlagen der Quantenmechanik* (Springer, Berlin, 1932) [E. T. Beyer, *Mathematical Foundations of Quantum Mechanics* (Princeton University Press, Princeton, 1955)].
[3] C. W. Helstrom, *Quantum Detection and Estimation Theory* (Academic, New York, 1976).
[4] E. B. Davies, IEEE Trans. Inf. Theory **IT-24**, 596 (1978).
[5] L. B. Levitin, in *Information Complexity and Control in Quantum Physics*, edited by A. Blaquiere, S. Diner, and G. Lochak (Springer, Berlin, 1987), p. 15.
[6] A. S. Kholevo, Prob. Inf. Transm. (USSR) **9**, 596 (1973).
[7] A. Peres, *Quantum Theory: Concepts and Methods* (Kluwer, Dordrecht, 1993), Chap. 9.
[8] A. K. Ekert, B. Huttner, G. M. Palma, and A. Peres, Phys. Rev. A **50**, 1047 (1994).
[9] J. M. Jauch and C. Piron, Helv. Phys. Acta **40**, 559 (1967).
[10] V. B. Braginsky and F. Y. Khalili, *Quantum Measurement* (Cambridge University Press, Cambridge, 1992), Chap. III.
[11] P. A. Benioff, J. Math. Phys. **13**, 231 (1972).
[12] A. Peres, Phys. Lett. A **128**, 19 (1988).
[13] M. A. Neumark, C. R. Acad. Sci. URSS **41**, 359 (1943).
[14] S. L. Braunstein and C. M. Caves, Found. Phys. Lett. **1**, 3 (1988).
[15] I. D. Ivanovic, Phys. Lett. A **123**, 257 (1987).
[16] B. Sz.-Nagy and C. Foiaş, *Harmonic Analysis of Operators on Hilbert Space* (North-Holland, Amsterdam, 1970).
[17] R. Loudon, *The Quantum Theory of Light* (Oxford University Press, Oxford, 1983).
[18] M. J. Messerly, R. E. Budewitz, B. K. Nelson, and R. C. Mikkelson, J. Light. Tech. **9**, 817 (1991).
[19] A. Muller, Ph.D. thesis, University of Geneva, 1996 (unpublished).
[20] N. Gisin, Opt. Commun. **114**, 399 (1995).
[21] P. C. M. Owens, J. G. Rarity, P. R. Tapster, D. Knight, and P. D. Townsend, Appl. Opt. **33**, 6895 (1994).
[22] N. Gisin, Phys. Lett. A **210**, 151 (1996).
[23] C. H. Bennett, G. Brassard, and A. K. Ekert, Sci. Am. **267** (4), 50 (1992).